

A Theory of DNA Dissociation from the Nucleosome

Nancy L. Marky and Gerald S. Manning*

Department of Chemistry
Rutgers, the State University
of New Jersey, New
Brunswick, NJ 08903, USA

Previous analysis of an elastic model of the nucleosome indicated that 10 bp end segments of DNA can exist in a continuum of mechanically stable trajectories ranging from complete winding on the histone octamer to complete unwinding. Stable states of 20 bp and 40 bp end segments, however, are grouped in bands separated by gaps where DNA trajectories are unstable. We extend these results to cover the entire range up to a complete nucleosomal turn, 80 bp. We find that 10 to 60 bp segments have states intermediate between fully wound and fully unwound that are mechanically stable. In striking contrast, there is no stable intermediate trajectory for 70 bp or 80 bp segments. Segments of these lengths constitute a two-state system. A 70 or 80 bp segment is either fully wound or fully unwound, and the population of these states is governed by Boltzmann's thermal distribution. We have found a plausible dissociation pathway from the fully wound to the fully unwound state for the 80 bp segment. In a ponderous breathing motion that breaks all contacts with the histone surface, the segment climbs to an activation peak of about 12 kcal/mol, then rapidly straightens away from the histone core to complete dissociation.

© 1995 Academic Press Limited

Keywords: nucleosome; activation energy; unfolding; conformational transitions

*Corresponding author

Introduction

A nucleosome core particle consists of a 146 base-pair (bp) fragment of DNA wrapped around an octamer of histone proteins in about 1.75 superhelical turns (van Holde, 1989). In the belief that in accessible experimental conditions, end segments of nucleosomal DNA of varying lengths can dissociate in response to changes in environmental variables like temperature and ionic strength (Simpson, 1979; Yager *et al.*, 1989), we have initiated development of a theoretical model for DNA dissociation from the protein surface (Manning, 1985, 1988; Marky & Manning, 1991). Since the 146 bp total length of core nucleosomal DNA is about equal to the persistence length of a DNA polymer, it seems reasonable that nucleosomal DNA, or any portion of it, can be modeled as a stiff rod with elastic bending energy. If the DNA-histone attractive interactions are sufficiently strong, a DNA end segment will be held to the protein surface against its tendency to straighten. But if the attractive forces are weakened (or if the stiffness of the DNA against bending is strengthened), the complex can dissociate.

We sought the minimum energy path of a DNA end segment as a function of the strength of the histone-DNA attractive force (Marky & Manning, 1991). That is, we looked for stable positions of the

end segment. Unsurprisingly, we found indeed that the segment is in stable position on the protein surface if the protein-DNA attraction is sufficiently strong. We found also that in the opposite extreme, when the histone-DNA attraction is weak, the end segment is stable only when fully dissociated, that is, when it has swung out straight from the curved protein surface. For histone-DNA attractive forces of intermediate strength, our results were less obvious and therefore more interesting. Intermediate attractive field strengths did not necessarily stabilize intermediate paths. Instead, depending on the length of the end segment, discontinuous behavior could be observed. A small change in the attractive field strength could induce a large-scale jump from one path to a distant path, a behavior reminiscent of the temperature transition found in Simpson's experiments (Simpson, 1979).

In our previous calculations, we looked only for the DNA path representing the absolute minimum energy. For given values of the histone-DNA attractive field and DNA rigidity, there is only one such path. But the existence of temperature means that there could be fluctuations, or breathing modes, in which end segments of the DNA come off the histone octamer and go back on again. To investigate this possibility requires consideration of secondary minima and activation energies, one of the topics to be explored in this paper.

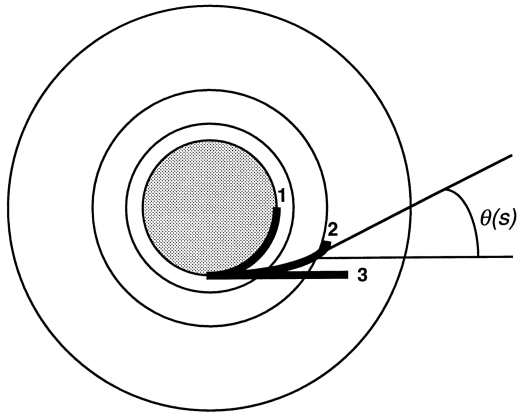


Figure 1. The geometrical description of the model. The shaded circle is the cylinder-like histone octamer, viewed by looking down on the cylindrical axis. Curves 1, 2 and 3 represent an end segment (tail) of DNA. Curve 1 represents a completely wound segment on the cylindrical octamer. Curve 3 is the same DNA tail when completely dissociated from the histone surface. Curve 2 is an intermediate path between curves 1 and 3. The thin circles are isopotential lines representing attractive histone-DNA forces. At arc length s along the path of the DNA, measured from the common starting point of the three curves, the angle of inclination of the path to the horizontal is designated as $\theta(s)$.

Yager *et al.* (1989) have made detailed measurements focused on another interesting aspect of nucleosome behavior, the complete dissociation of the intact core particle to free DNA and unbound proteins. They found substantial reversible dissociation to free DNA at salt concentrations below 0.75 M. The percentage of free DNA increases as a function of salt concentration, reaching a value of about 24% at 0.75 M NaCl. The dissociation between 0.1 M and 0.75 M salt apparently involves a two-state mechanism; intermediate states could not be detected. The all-or-none behavior observed below 0.75 M contrasts with the dissociation process in the range 0.8 M to 1.5 M NaCl, where an intermediate species in which the DNA has only partially unwrapped (and histones H2A and H2B have been lost) is also found.

A question raised by these experiments is why histone-DNA dissociation proceeds differently at low and high salt, directly to free DNA in the former case, indirectly *via* a stable intermediate in the latter. We propose here that low-salt dissociation is driven by an all-or-none elastic response of the DNA, whereas at high salt, DNA has lost a substantial part of its elastic resiliency and unwinds more in analogy to a flexible thread than to a stiff rod.

Description of the Model

General description

The histone octamer presents a cylindrical surface to the DNA wound around it (Arents & Moudrianakis, 1993). In Figure 1 we look down

along the axis of the cylinder. An end segment of the DNA is shown in three possible trajectories. It is a circular arc when entirely wound on the cylindrical octamer. It is a straight line extending out from the cylinder when completely dissociated (except for its internal end point, which remains attached to the protein). The intermediate path represents an intermediate state between complete winding and complete dissociation. All three trajectories proceed from a common anchoring point, which in the real system would correspond to a discrete patch of histone-DNA contacts. If the “end segment” is a half-segment of nucleosomal DNA, the anchoring point is at the dyad axis.

The intermediate trajectory in Figure 1 as well as the completely wound path are assumed to possess positive Hooke’s law elastic bending energy:

$$E_{\text{bend}} = \frac{1}{2} b \int_0^L \kappa^2 ds, \quad (1)$$

where b is the Hooke’s law constant for bending, s is arc length along the DNA segment measured from the point of attachment in Figure 1, κ is the curvature of the segment at position s , and L is the length of the segment. Equation (1) takes the intrinsic curvature of the DNA as zero. We will consider the effect of sequence-directed intrinsic curvature (Shrader & Crothers, 1989) in another paper.

Since the partially and fully wound paths have positive bending energy, the DNA in either trajectory would spontaneously straighten toward the completely extended trajectory were it not for a competing effect, namely, the attractive interaction with the histone surface, which endows it with a component of negative energy:

$$E_{\text{histone-DNA}} = -\gamma \int_0^L w ds \quad (2)$$

In this expression, the amplitude γ measures the strength of the attractive histone-DNA interaction, and the function $w(s)$ gives its distance dependence. More precisely, $-\gamma w(s)ds$ is the attractive energy of a cross-section of DNA of thickness ds located at arc length s along the DNA, and the integral along the DNA length gives the total attractive energy.

We use a simplified representation of w . Let r_0 be the radius of the shaded disk in Figure 1 (i.e. the radius of the histone octamer). Let r be the radial distance of a point on a DNA trajectory (at arc length s) to the center of the shaded disk. Then the difference $r - r_0$ is the distance of a point on the DNA to the surface of the histone octamer. Define a dimensionless measure of this distance:

$$\rho(s) = \frac{|r - r_0|}{r_0} \quad (3)$$

For w we then use the function:

$$w(s) = e^{-\delta\rho^2/2} \quad (4)$$

The representation of w given by equation (4) defines a ring, or trough, of negative potential energy

with parabolic cross-section (for small ρ) centered along the circle in Figure 1 that bounds the shaded disk. The potential energy minimum is located on the circle, i.e. at the surface of the octamer, at $r = r_0$. In effect, we replace the octamer by this ring of potential energy. The dimensionless parameter δ measures the effective width of the potential energy ring. In Figure 1 the potential energy ring outside the histone octamer is represented by concentric isopotential circles; the attractive energy becomes smaller with increasing distance. With the exception of the completely associated trajectory, possible DNA paths cut the isopotentials obliquely, as exemplified by trajectories 2 and 3 in Figure 1, resulting in complex behavior.

The ring of potential energy is uniform in the present model. In subsequent work, but not here, a more realistic potential function will be used, in which the discrete, predominantly ionic, histone-DNA contacts will be recognized. Explicit inclusion of ionic forces will allow us to explore the effect of asymmetric neutralization of the phosphate charge in the context of the nucleosome complex (Mirzabekov & Rich, 1979; Manning *et al.*, 1989; Strauss & Maher, 1994).

There is a third source of energy changes in this system, the twist of the DNA. To bind specifically to protein residues on the histone surface, the DNA must be torsionally in register. Part of the DNA is overwound, and part is underwound (Hayes *et al.*, 1990). Estimates based on the twisting data presented by Shore & Baldwin (1983) indicate that the effect of the resulting twisting stresses in terms of energy is about 3 kcal/mol per turn of DNA around the histone core, or about 15% of the bending energy. The twisting energy, therefore, although significant, can perhaps be provisionally overlooked for the sake of simplicity in an initial model. Finally, our model assigns no role to the N-terminal tails of the core histones, which do not affect DNA dissociation behavior (Ausio *et al.*, 1989).

The model may be used in various ways. One way to use it, for example, is to minimize the total energy $E_{\text{bend}} + E_{\text{histone-DNA}}$ for different values of γ (the depth of the potential energy ring). We would then find the stable DNA path for different depths of the energy ring. If the ring is very deep, we would expect the minimum-energy path to run along the bottom of the ring, that is, the DNA would be completely associated with the octamer and in contact with it along its entire length. If the ring is flat (no histone-DNA attraction), then the minimum energy path would extend straight out from the octamer to minimize the bending energy. For intermediate depths, it is hard to make predictions in advance of the calculated results. It may be appreciated that the energy of a given trajectory is given by integrals along its entire length. The attractive energy near the end of the segment is, in general, as important as the bending energy near the beginning.

The definition of a parameter g is useful in correlating our results. We refer to it loosely as the "binding strength ratio". When it is large, the DNA

segment is wound onto the histone octamer. When it is small, the DNA segment is unwound from the protein surface. Our definition is:

$$g = \frac{\gamma}{(1/2)br_0^2} \quad (5)$$

If the numerator and denominator of this expression are both multiplied by the length L of the DNA segment, the precise meaning of g becomes clear. Noting that $w = 1$ in equation (2) when $r = r_0$, we see that g is the ratio of the histone-DNA attractive energy when the DNA segment lies entirely on the histone surface to the elastic bending energy of the DNA segment in the same circumstance. Values of g near unity have special significance. When $g = 1$, the total energy (bending plus histone-DNA interaction) of a DNA segment lying entirely on the histone surface equals zero. But the fully extended segment also has total energy near zero (the bending energy vanishes for the straight segment, and the histone-DNA attraction is significant only near the point of attachment, most of the extended segment lying far from the histone octamer). Thus, when $g = 1$, the two extreme possibilities for the DNA trajectory (see Figure 1) have nearly the same energy.

The integrals in equations (1) and (2) are taken along the trajectory of the DNA segment. Therefore, we need a mathematical representation of the trajectory. For example, we have used a two-parameter family of trajectories for many of our calculations:

$$\theta(s) = x_1(s/L) + x_2(s/L)^2 \quad (6)$$

The angle of inclination θ is indicated in Figure 1; it defines the shape of the trajectory as it varies along its length. The two parameters are x_1 and x_2 . Assigning specific numerical values to these parameters produces a specific trajectory. If $x_2 = 0$, the trajectory is the arc of a circle. Negative values of x_2 allow the arc to straighten near its end. For given values of x_1 and x_2 , the energy integrals in equations (1) and (2) are evaluated numerically.

The algorithm in detail

In this subsection we give a more systematic presentation of the procedure used to calculate the energy of a DNA trajectory. A specific trajectory is chosen by assigning numerical values to the coefficients x_i and the index N in the trajectory representation:

$$\theta(s) = \sum_{i=1}^N x_i \left(\frac{s}{L}\right)^i \quad (7)$$

In this equation L is the length of the trajectory (the DNA segment), and s is the arc length along the trajectory. The angle θ is defined by the direction of the trajectory at s and the horizontal u -axis, as indicated in Figure 1 and its legend. The elastic energy integral in equation (1) is immediately computable, since the curvature $\kappa(s)$ is equal to $d\theta/ds$.

Numerical computation of the histone-DNA attraction energy integral in equation (2) is accomplished with the aid of formulas for the (u, v) Cartesian coordinates of the DNA trajectory:

$$u(s) = \int_0^s \cos \theta \, d\theta, \quad v(s) = \int_0^s \sin \theta \, d\theta \quad (8)$$

These coordinates are substituted into the following formula for $\rho(s)$ in equation (4):

$$\rho = \left[\left(\frac{u}{r_0} \right)^2 + \left(\frac{v}{r_0} - 1 \right)^2 \right]^{1/2} - 1 \quad (9)$$

and the result for $w(s)$ is used to compute the integral in equation (2).

We factored b out of the sum $E_{\text{bend}} + E_{\text{histone-DNA}}$, thus obtaining the ratio g defined in equation (5); and see equations (1) and (2). The minimum energy trajectory (that with minimum $E_{\text{bend}} + E_{\text{histone-DNA}}$) is reported for a fixed value of g . Numerical values of the parameters b , r_0 , and δ approximating the nucleosomal core particle system were chosen as described by Marky & Manning (1991).

Scanning the System for Stable Structures

We have previously produced an explicit formula for the stable equilibrium path (the one with globally minimum energy) of a very short DNA segment as a function of the binding strength ratio g (Manning, 1985). The equilibrium trajectory is then a circular arc that gradually winds onto the histone cylinder as g increases. The numerical procedure discussed above verified this result for a 10 bp segment, but revealed discontinuous behavior for longer segments (Marky & Manning, 1991). At critical values of g , the stable equilibrium path jumps from a position relatively far from the histone surface to a position relatively close.

We analyzed previously the cases of 10, 20, and 40 bp segments (Marky & Manning, 1991). We have extended these results, so that we now have data for 10, 20, 30, 40, 50, 60, 70, and 80 bp segments. Eighty base-pairs corresponds to about a complete turn of DNA around the histone octamer. Seventy base-pairs is about half the length of nucleosomal core particle DNA, the two halves being symmetrically disposed. The symmetry of the nucleosome structure implies that if the energy-minimizing conditions are such that one turn is completely unwound, then the other turn is also completely unwound. Thus, we interpret the complete unwinding of a 70 or 80 bp segment as implying the dissociation of the nucleosome into free DNA and protein.

Figures 2 through 9 show the complete set of results. Each Figure corresponds to a DNA segment of given length. The first part of each Figure, designated (a), shows the actual stable equilibrium trajectories, labeled with corresponding values of

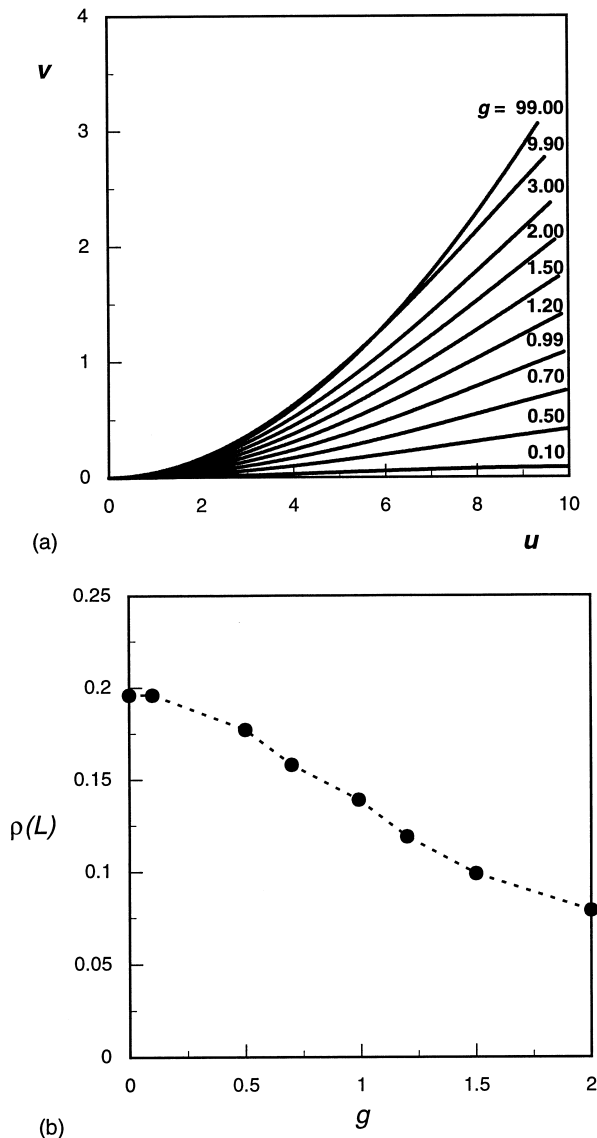
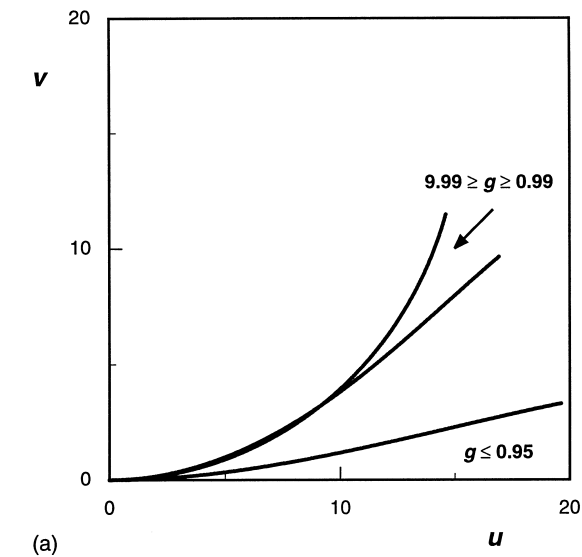


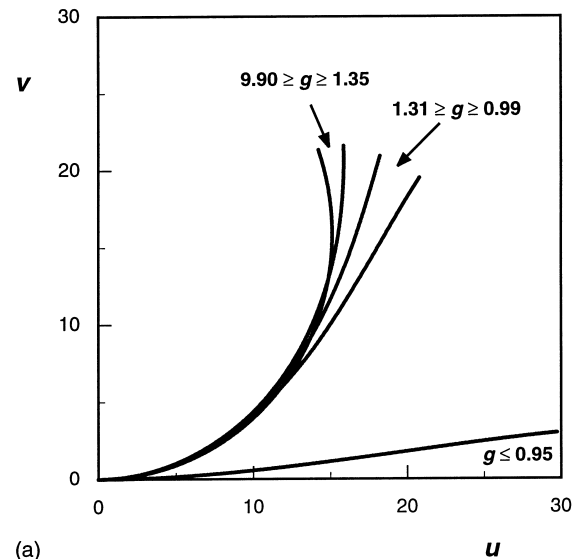
Figure 2. (a) Minimum-energy paths for a 10 bp DNA tail. The view is from above, as in Figure 1. The quantity g is a measure of the strength of the histone-DNA forces relative to the stiffness of the DNA. As g increases, the 10 bp tail is continuously drawn toward the histone surface. The coordinates u and v are ordinary planar cartesian, measured in units of base-pairs of DNA, 3.4 Å/bp. (b) The reduced radial distance $\rho(L)$ of the end point of the DNA tail from the histone surface as a function of g . There is a smooth decrease in $\rho(L)$ as g is increased. The maximum value of 2 for g is to emphasize the DNA behavior at different chain lengths, as will be seen in the following Figures.

the binding strength ratio g . The second part of each Figure, designated (b), is a plot of $\rho(L)$ as a function of g . That is, with reference to equation (3), the reduced radial distance of the end-point of the segment, in its stable equilibrium path, is plotted against the binding strength ratio.

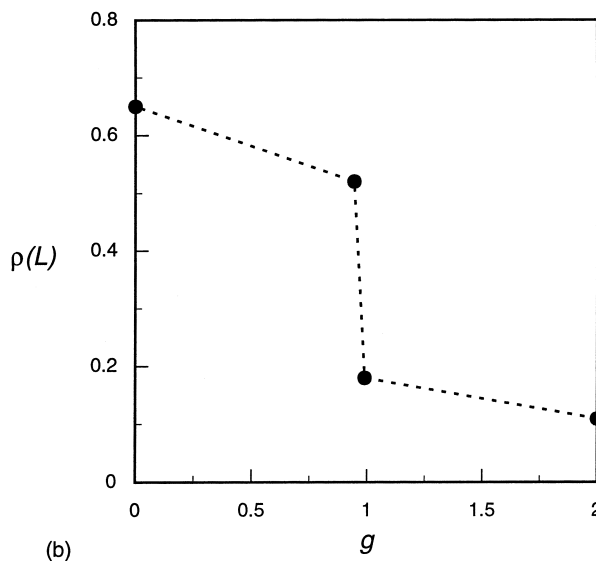
Figure 2 shows the continuous winding of a short (10 bp) segment as the binding strength increases. Figures 3 through 9 show varying degrees of all-



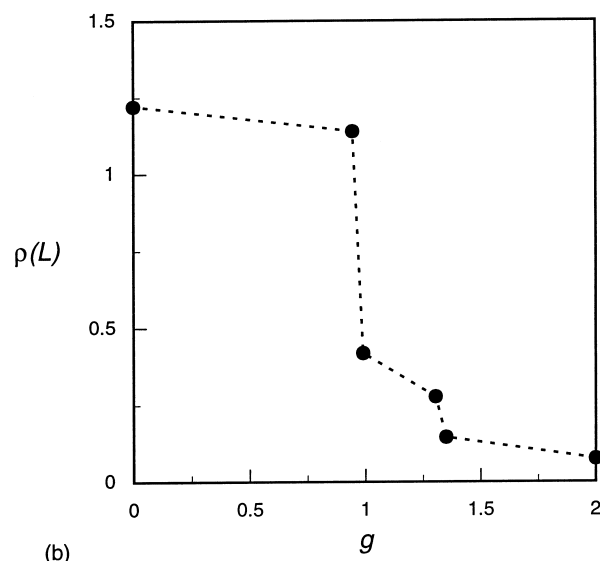
(a)



(a)



(b)



(b)

Figure 3. (a) Behavior of a 20 bp DNA tail. The $g = 9.90$ curve is on the histone surface. As g decreases to a value near unity, the DNA is progressively released, but remains close. It then jumps to a position far from the surface, and continues gradually toward complete dissociation as g approaches zero. The paths are divided into two continuous bands, with the indicated g values as their boundaries. (b) The filled circles represent the paths at the extremes of the bands. The abrupt release of the tail near a g value of unity is clearly seen. The behavior of the 20 bp tail contrasts with that of the 10 bp tail (Figure 2(b)).

Figure 4. (a) A 30 bp DNA tail has a new jump when g is 1.31, now, separating the band for $g = 0.99$ to 9.90 into two sub-bands (compare this result with the 20 bp behavior in Figure 3(a)). (b) This second gap is better seen in the $\rho(L)$ versus g plot.

or-none behavior. In Figure 3 a 20 bp segment is observed to jump at $g = 1.0$ from a trajectory relatively far from the protein surface to a path relatively near. However, the near path at $g = 1$ is not fully wound on the cylinder; a gradual progression through intermediate paths leads to complete winding as g increases from 1 to 10. In Figure 4 for 30 bp, two jumps are evident. The first, from far to near, is at $g = 1.0$; the second is at $g = 1.3$ and carries the segment still closer to the surface. The jumps are possibly more clearly seen from the representation

in Figure 4(b). There are many intermediate states between $g = 1.0$ and 1.3 and between 1.3 and 10.

In Figure 5 a “tightening up” is observed for 40 bp. There is only a narrow band of intermediate paths after the first jump, and the segment is all but fully wound after the second jump. Figures 6 and 7 show continuation of the narrowing trend for 50 and 60 bp. We continue to find two jumps, but the intermediate state consists (for practical purposes) of a single trajectory, and the segment is fully wound immediately after the second jump. At 70 bp we fail to find any intermediate state, nor is an intermediate state found for 80 bp; for practical purposes, a single jump at $g = 1.1$ in Figures 8 and 9 carries the corresponding segment from a completely unwound trajectory to its native, fully wound configuration.

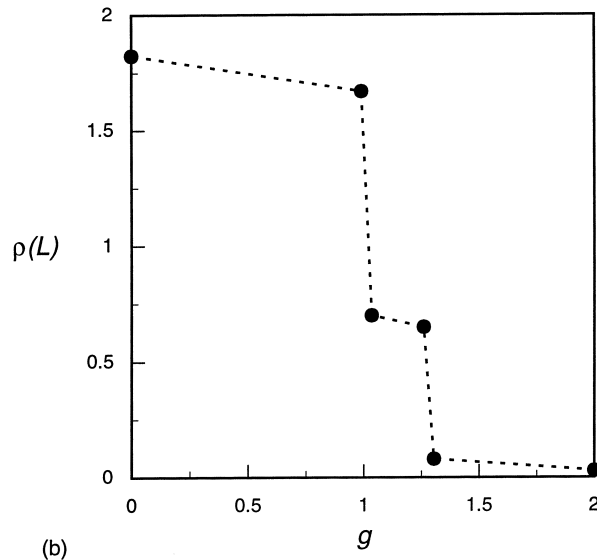
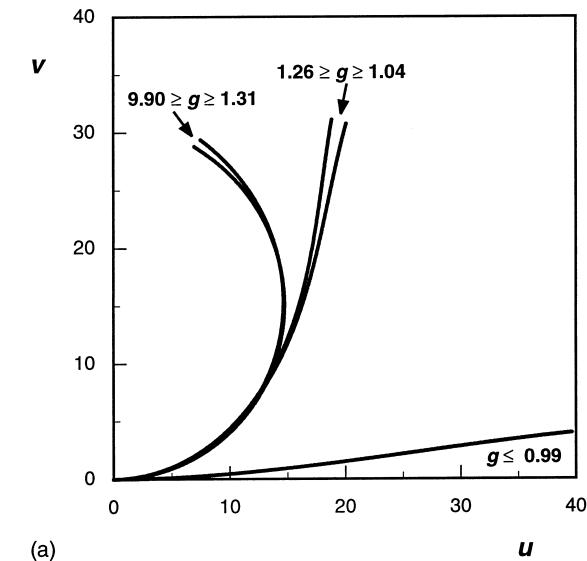


Figure 5. (a) The “tightening up” of the two bands close to the histone surface is manifested by the 40 bp DNA tails. The DNA stays essentially associated with the histone surface down to a value of 1.31. At this value of g a segment of about 20 bp dissociates from the surface. (b) This second jump has a larger gap in $\rho(L)$ than for the 30 bp tail, but at the same time the two jumps occur in a narrower range of g , around unity.

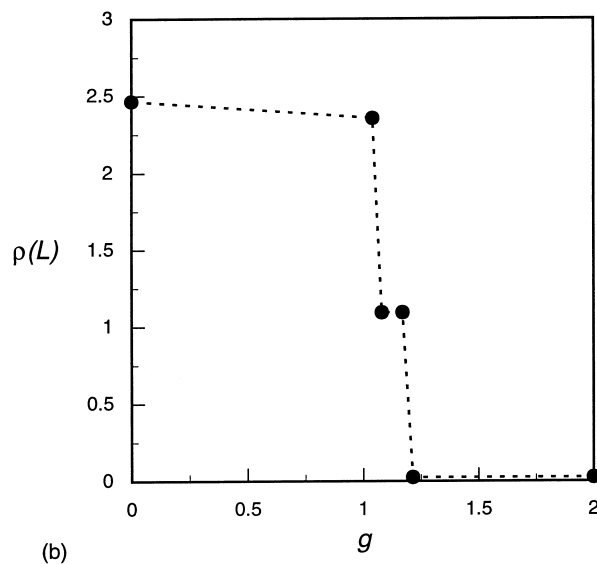
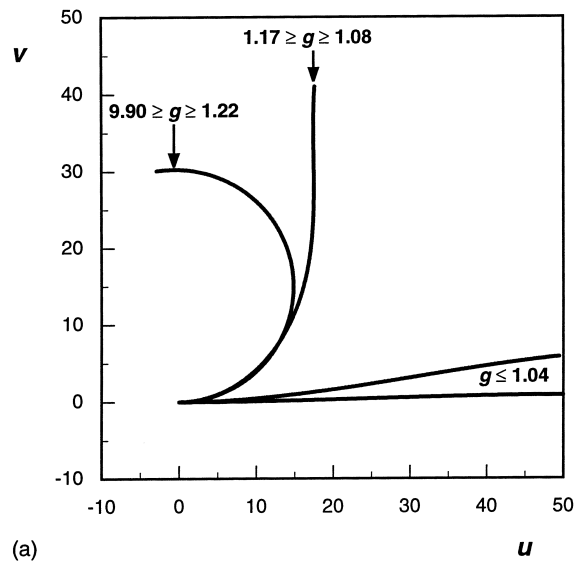
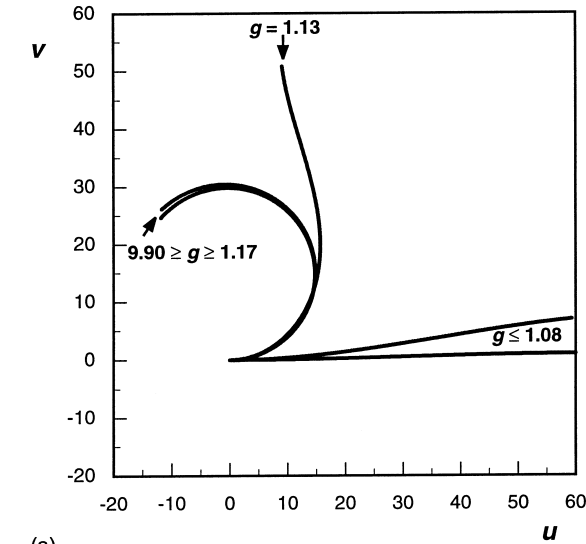


Figure 6. (a) The 50 bp DNA tail narrows even more the bands between the two jumps. The minimum-energy trajectories for $g = 1.08$ to 1.17 are indistinguishable in this two-dimensional space treatment. These trajectories are now precisely separated in space from the completely wound and the completely unwound DNA. (b) With respect to the change in $\rho(L)$ values, the two gaps in $\rho(L)$ become comparable in size. The range of g values at the jumps is smaller.

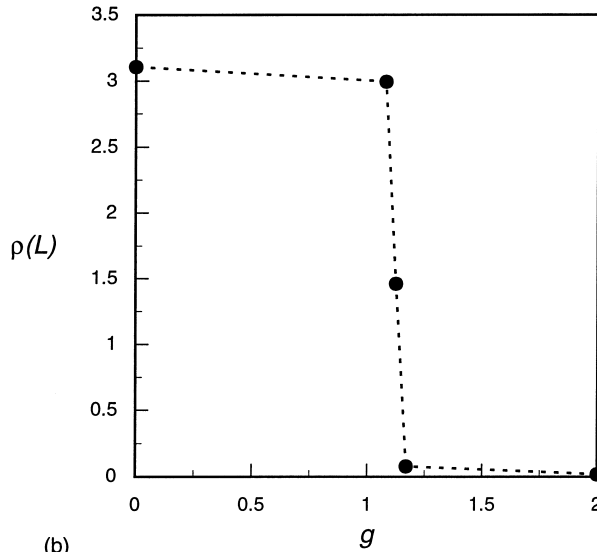
Let us consider the implications of the results for 70 and 80 bp. We find a jump at $g = 1.1$ between fully wound and fully unwound states. There is no intermediate state. The energies of fully wound and fully unwound states are nearly equal at the jump point. The Boltzmann distribution then dictates that these two states are almost equally populated, while no intermediate state is available. In the experiments of Yager *et al.* (1989), the fraction of particles in the unwound state (fraction of free DNA), although less than 50%, is substantial. No intermediate state is observed. We suggest that our model corresponds to the conditions of the experiments with g slightly

greater than 1.1. In native conditions, the experiments, and our model, indicate that the core particle is barely stable.

In summary of this section, we have scanned our system for stable structures by varying the binding strength ratio g and looking for the unique, globally least-energy trajectory of an end segment of DNA. We find states intermediate between fully wound and fully unwound for segments of length less than 70 bp. We do not observe an intermediate state for 70 or 80 bp segments. Instead, when g decreases, a critical value is reached when complete unwinding abruptly proceeds from a fully wound state.

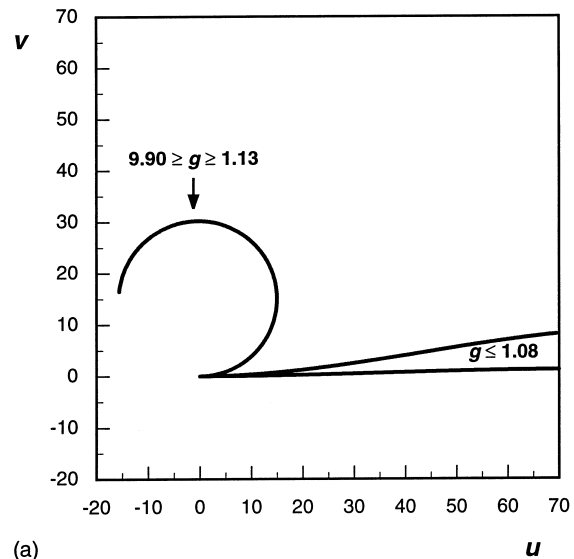


(a)

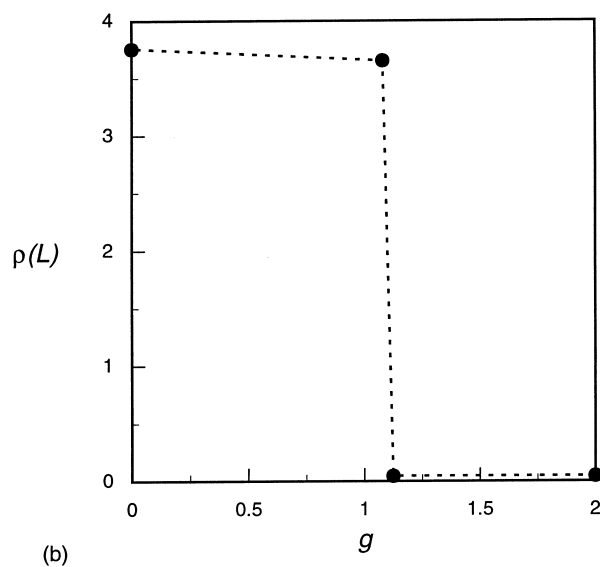


(b)

Figure 7. (a) The behavior of the 60 bp segment is even more dramatic than that of the 50 bp tail; it is only one intermediate path, for the value of $g = 1.13$. (b) The two jumps are collinear with that unique trajectory almost half-way in $\rho(L)$ values.



(a)



(b)

Figure 8. (a) The 70 bp pair segment has no intermediate state in its dissociation from the histone surface. The DNA is fully wound or unwound at g values of 1.13 and 1.08. (b) The complete dissociation occurs at g about 1.1.

Dynamic Dissociation of the 80 bp Segment

In this section we investigate the behavior of the 80 bp segment at a fixed value of the binding strength ratio g . For reasons shortly to be explained, we choose the numerical value $g = 1.2$, which is slightly greater than the critical jump value 1.1. We see from Figure 9 that the minimum energy path for $g = 1.2$ is fully wound on the histone cylinder. Any partially or fully unwound trajectory has higher energy if g is fixed at 1.2. We also learned from Figure 9, however, that the fully unwound path represents the globally minimum energy for a value of g only slightly less than 1.2. This result suggests that when $g = 1.2$, the fully unwound path will have only a slightly higher energy than the fully wound

path. In this case, the existence of temperature and the Boltzmann distribution would guarantee a substantial equilibrium population of fully unwound, hence free, DNA. In fact, if $g = 1.2$, we calculate the energy of the fully unwound trajectory as about 2 kcal/mol higher than the fully wound path, so that the equilibrated Boltzmann ratio of fully unwound to fully wound states at room temperature is about 3%, similar to what Yager *et al.* (1989) find at physiological ionic strength. It is for this reason that we have chosen $g = 1.2$ for our numerical example; it apparently corresponds to the native histone-DNA binding energy in physiological salt conditions.

Yager *et al.* (1989) extended their measurements to the kinetics of dissociation. If the salt level was initially sufficiently low that nearly all core particles were intact, and salt was then jumped to a higher

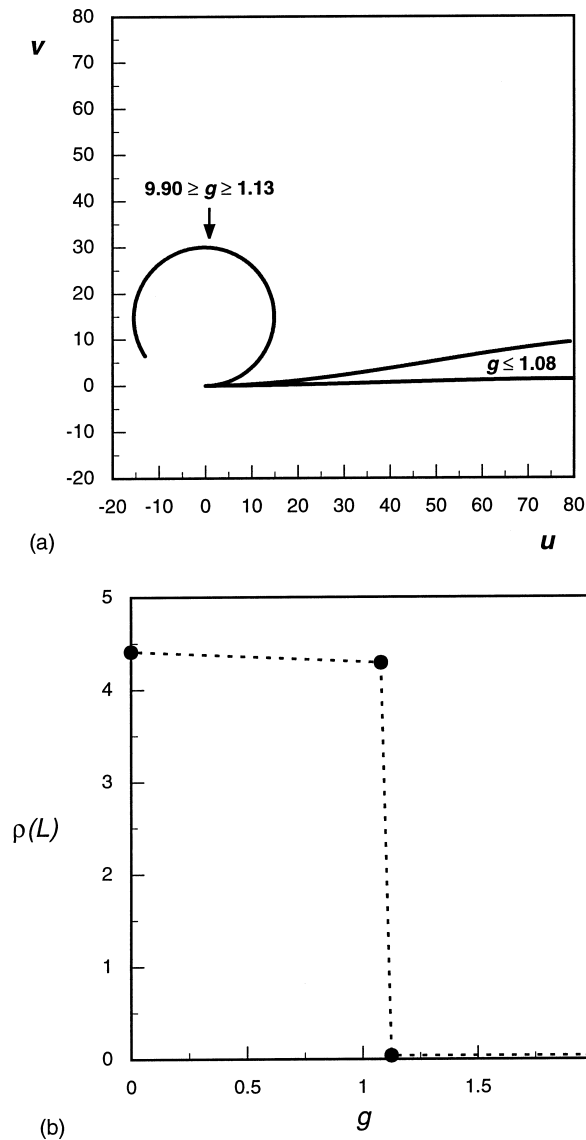


Figure 9. (a) The 80 bp DNA segment has only two states, with the same values of g as the 70 bp segment. (b) The DNA undergoes complete dissociation at g about 1.1, just like the 70 bp segment in Figure 8(b).

level where the equilibrium fraction of dissociated particles was substantial, the approach to equilibrium was observed to be slow. The dissociated state has energy only slightly higher than the intact state, but a large activation energy must separate these two states, which coexist in dynamic equilibrium. No intermediate state, such as DNA bound to a hexamer of histones, was observed. It seems to us that a high activation energy separating two extreme states, fully native and fully dissociated, with no intermediate state, is most easily explained by a mechanism containing a step in which nearly all histone-DNA contacts are simultaneously broken. This all-or-none high-energy step would be followed by complete disruption of the core particle, allowing no possibility of intermediate products. Our model can in fact generate a dissociation pathway of this type with about a 12 kcal activation

energy. An alternative mechanism involving contact-by-contact peeling of the DNA from the protein core is described in Discussion, but skeptically, because we would expect it to lead to the formation of observable intermediates. By the same token, however, peeling could underlie the dissociation behavior at high salt, when intermediate products are observed.

We begin our derivation of the all-or-none dissociation mechanism. Starting with the fully wound trajectory at $g = 1.2$, the 80 bp DNA segment must pass through a continuum of trajectories, all with the fixed value $g = 1.2$, in order to straighten away from the histone core to its fully dissociated trajectory. To get a feeling for the situation across the whole pathway from fully folded to fully unwound states, we first plot circular trajectories. The first-order parameter x_1 in equation (6) is varied from the value 5.333 to zero, while x_2 is fixed at zero. Each value of x_1 then produces an arc of a circle. The value 5.333 corresponds to a circle coinciding with the surface of the histone core; this trajectory is the fully wound state with all protein-DNA contacts realized. Smaller values of x_1 give circular arcs with radii larger than the radius of the histone octamer. Therefore, except at the dyad axis, all contacts with the histone core are simultaneously broken at the outset of dissociation. The energy course of the dissociation pathway through circular trajectories is illustrated by Figure 10(a). An activation energy of about 12 kcal for a trajectory lying close to the histone core is prominent. In Figure 10(b), we show the fully wound trajectory and the “activated” trajectory, the one at the top of the activation peak. We interpret the activated trajectory, which is apart from, but close to, the histone surface, as having all contacts with the histones broken. Circular trajectories further out than the activated trajectory are unstable, as we proceed to show.

It is possible that the attractive potential is not strong enough to sustain the uniform curvature of a circular trajectory near its end, where the distance from the histone surface is greatest and the attractive forces weakest. To check this eventuality, we broadened the class of possible trajectories to include those with negative values of x_2 . It is clear from equation (6) that such trajectories straighten away from circularity as the end is approached. We found all trajectories to the left of the activation peak in Figure 10(a), the “near” trajectories, to be quasi-stable in the sense that for a given value of x_1 , the corresponding circular trajectory, with $x_2 = 0$, has minimum energy among all trajectories with the same value of x_1 and $x_2 \leq 0$. In other words, in the climb up the activation energy hill, which corresponds physically to the simultaneous breaking of histone-DNA contacts, the circular trajectories have no tendency to straighten. This situation is prototypical in the description of a kinetic process with the aid of an energy surface. The climb to the activation energy peak with circular trajectories proceeds uphill along the floor of an energy valley.

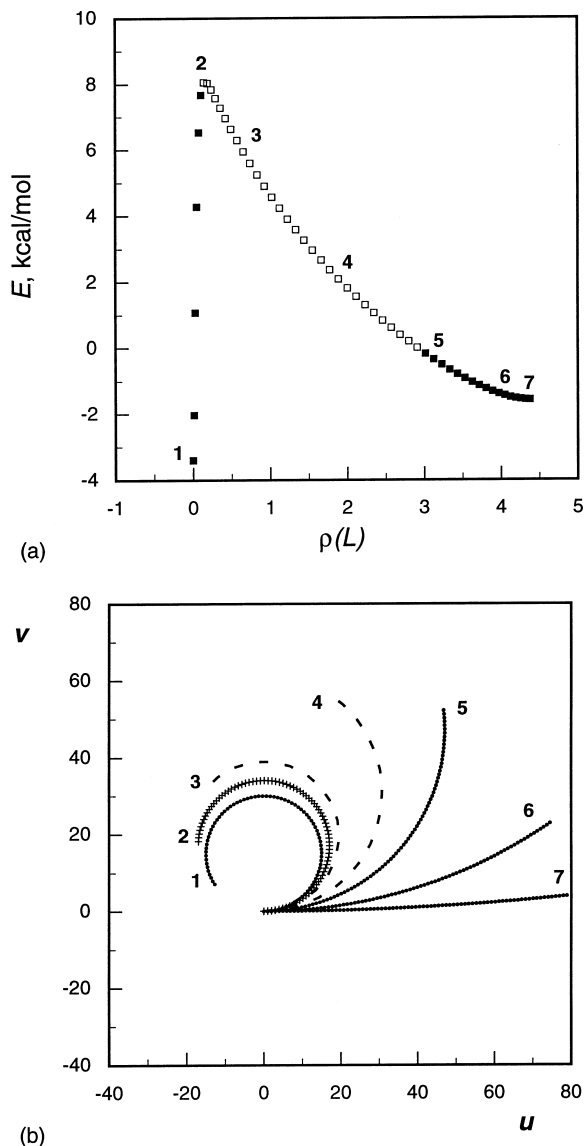


Figure 10. (a) The energy profile for the dissociation of the 80 bp segment of DNA along circular trajectories, in kcal/mol. The value of g is fixed at 1.2. These trajectories have the free end located at the specified value of $\rho(L)$, the reduced radial distance from the histone surface. As discussed in the text, the filled squares follow a stable pathway, while the open symbols trace an unstable energy ridge. (b) The trajectories corresponding to the energy profile in (a). The cross-hatched trajectory is “activated”; it corresponds to the peak energy in (a). The broken circular trajectories are strongly unstable, as discussed in the text. The energies of the numbered trajectories are indicated by the corresponding number in (a).

The energy landscape changes dramatically once the activation peak is attained. The “far” circular trajectories in Figure 10(a), those to the right of (and including) the activated trajectory, are not stable against straightening. For a fixed value of x_1 characterizing one of these circular-arc trajectories, trajectories with negative values of x_2 have lower energy than the circular arc with vanishing x_2 . The descent from the peak toward complete dissociation, on the far side in Figure 10(a), is unstable. Proceeding with

circular trajectories, as in Figure 10(a), travel would be along an energy ridge. The least fluctuation sends the DNA falling from the ridge along a series of trajectories rapidly straightening away from circular shape. Finally, as indicated in the legend to Figure 10, circular trajectories of very large radii of curvature, corresponding to nearly complete dissociation of the DNA, regain much of their stability toward straightening.

We recapitulate these results for the two-parameter family of trajectories given by equation (6) with zero or negative values of x_2 . The native structure continually undergoes a ponderous breathing motion in which protein-DNA contacts are broken along the entire length of the DNA, except at the dyad axis, then reformed. In this motion the DNA is never far from the histone surface. Breathing would be represented in Figure 10(a) by an uphill climb toward the activation peak followed by a fallback. In the relatively rare event of a breathing movement of amplitude large enough to carry the DNA to the top of the peak, instability ensues. The DNA then rapidly straightens away from the histone core to complete dissociation.

For dissociation in the real system, the instability would actually be stronger than in our model. For once histone-DNA contacts are broken, the stressed twist of the DNA relaxes, and the DNA falls out of twist register with its protein contacts. The attractive histone-DNA energy falls to small values more abruptly than in our model, and the only mechanical option for the DNA is to straighten away from the histone surface in a correspondingly more abrupt way.

Discussion

The model studied in this paper has severe limitations. It cannot give much insight into the structural changes that may occur in the binding site at the dyad axis. The nucleosome core particle has two halves, and our focus has been on the behavior of half of the overall nucleosomal DNA segment. The measurements reported by Yager *et al.* (1989) suggest that both halves of the DNA unwind together. If they did not, if only one moiety unwinds while the other remains wound, stable intermediates would presumably be observable, possibly a histone hexamer with a full complement of DNA, half of which would be in a native-like conformation, the other half “dangling.” That intermediates are not observed suggests that the decreased DNA curvature at the dyad axis, which must be a feature of the breathing movement illustrated in Figure 10(b), cannot be unilateral. Local structural symmetry at the dyad is perhaps not restricted to the native form. Perhaps decreased curvature on one side destabilizes the other side and results in decreased curvature there as well. Since the local structure of DNA is stiff, it is stiff at the dyad axis as well as elsewhere, and it is not unreasonable to invoke structural constraints there that would not allow the two DNA halves to move independently. It is difficult to

discuss this matter in any detail on the basis of a model that reduces the molecular structure of the site at the dyad to a mathematical point. In any event, to explain the absence of intermediates in DNA dissociation, we have to postulate that both halves of the DNA breathe outward simultaneously, breaking contacts with the histone core except at the dyad axis.

Even if both halves of the DNA unwind together, there is still attachment at the anchoring site on the dyad axis. We may suppose that DNA completes its dissociation to the protein-free state as a consequence of its dynamic equilibrium with the single remaining binding site at the dyad axis.

The histone octamer at low ionic strength is not stable. We have not considered the breakup of the octamer in our dissociation mechanism. Perhaps dissociation of the octamer occurs after dissociation to free DNA and is irrelevant to the DNA dissociation steps. If, for example, a histone dimer were to come off as an integrated part of the DNA dissociation mechanism, it would be hard for us to understand why intermediate products are not observed. A related point is that the attachment of the DNA ends to the H2 dimers is thought to be weak (Simpson, 1979; McGhee & Felsenfeld, 1980). It seems to us that the simplest interpretation of the dissociation data is all-or-none two-state dissociation of DNA from the intact octamer.

We have also not considered the possible effect of repulsion between the two halves of nucleosomal DNA (but see the discussion in Marky & Manning, 1991). Again, we feel that observable intermediate products would result from a mechanism in which half of the DNA dissociated under the driving influence of repulsion from the other half. For then, after dissociation of the first half, the second half would lack a driving force for dissociation.

We have discussed in some detail an all-or-none DNA dissociation mechanism centered on an initial high-energy breathing movement that breaks and reconstructs nearly all histone-DNA contacts simultaneously. Perhaps a more obvious mechanism would have the DNA peeling from the ends, sequentially breaking contacts one by one. We can simulate this dissociation pathway in the following way. Consider the subfamily of two-parameter trajectories in equation (6) for which the parameter x_1 is fixed at the value 5.333, while x_2 passes through increasingly negative values, starting at zero. The trajectory $(x_1, x_2) = (5.333, 0)$ coincides with the histone surface. A trajectory $(5.333, x_2)$ with $x_2 < 0$ begins with the same curvature as the histone surface but "peels" away from the surface as it proceeds. In Figure 11(a) we show the energy profile as peeling progresses; Figure 11(b) shows the trajectories themselves. There is an activation energy peak of about 8 kcal, but on the far side of the peak, there is a continuum of partially peeled trajectories all with energies within about 4 kcal of each other. We do not expect this mechanism to give rise to the observed all-or-none dissociation behavior. For example, trajectory 5 in Figure 11(b) retains exten-

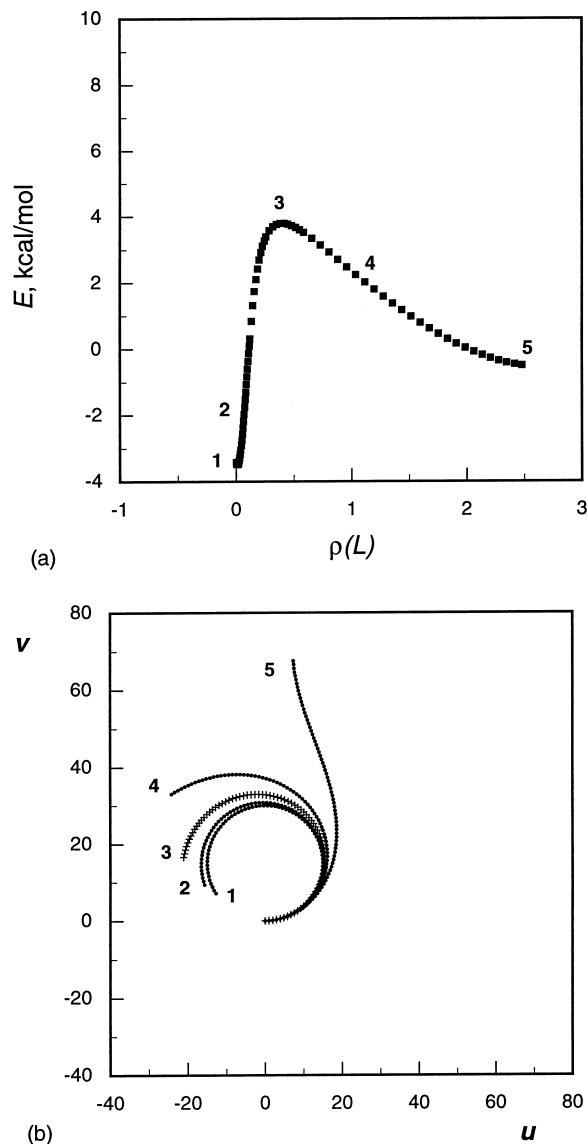


Figure 11. (a) The energy profile of a peeling mechanism, as described in the text. (b) The trajectories corresponding to the energy profile in (a).

sive contact with the histone surface but is only 2 kcal higher in energy than a fully unwound trajectory. It would be significantly populated at room temperature and could correspond to an observable intermediate.

We do not believe that the peeling mechanism is utilized for core particle dissociation, because we expect it to lead to a significant concentration of intermediate products, at variance with observation. But then a question arises. Why is this mechanism not realized in core particle dissociation? Indeed, in our model, it has a lower activation energy than all-or-none dissociation. The answer would have to involve considerations that we have not modeled. One possibility recognizes that "peeling" of DNA in the actual core particle implies sequential breaking of discrete contacts. DNA is a stiff molecule. Its structure may preclude the kinking at an unbroken

contact required to accommodate breaking of an adjacent contact. Deeper understanding may require all-atom energy computations.

Finally, we offer some qualitative discussion of the high-salt dissociation behavior observed by Yager *et al.* (1989). In the salt range 0.1 M to 0.75 M NaCl, these authors found the characteristics that have been emphasized in this paper; DNA dissociates to the free state in a cooperative all-or-none fashion, with no observable intermediate. We have attributed this sharp dissociation to the elastic resilience of 70 to 80 bp segments of DNA toward bending. Actually, as salt increases, there is good evidence that the persistence length of DNA diminishes (Frontali *et al.*, 1979; Manning, 1981; Borochoy, *et al.*, 1981; Cairney & Harrington, 1982; Eisenberg, 1990; Sobel & Harpst, 1991; Porschke, 1991; Nordmeier, 1992). The persistence length is proportional to the Hooke's law bending modulus b in the definition of g , equation (5). But the histone-DNA attractive energy is largely ionic, and therefore γ in equation (5) is also expected to decrease, leaving g roughly unchanged. The implication is that as salt increases, the dissociation behavior of the core particle may not change, in accord with observation up to about 0.75 M salt.

We can make this argument slightly more quantitative by comparing the 70 to 80 bp nucleosomal DNA segment with the persistence length as measured by Sobel & Harpst (1991). In the range 0.1 M to 1 M salt these authors report persistence lengths decreasing from 162 to 132 bp. A 70 to 80 bp segment is substantially shorter than these values, and may be supposed to withstand thermal fluctuations and thus behave elastically. Our results may apply throughout this salt range, the more tenuously at the high end.

Above 0.75 M salt, up to 1.5 M, the dissociation as observed is not so cooperative, and intermediate species are seen. A consistent explanation of the high-salt behavior would run as follows. Sobell & Harpst (1991) report persistence lengths that continue to decrease at high salt, from 132 bp at 1 M to 112 bp at 3 M. Persistence lengths in this salt range are thus greater than the length of a 70 to 80 bp segment, but perhaps not sufficiently so to prevent the segment from succumbing to thermal fluctuations and behaving more like a flexible polymer than like a rigid elastic rod. Dissociation would then proceed in the manner expected of a flexible chain. One segment can be freed with no resultant stress on an adjacent part, which then remains bound. Intermediates are then expected, and observed. In fact, the peeling behavior that we have rejected as a likely dissociation mechanism below 0.75 M salt could underlie the experimental observations at higher salt.

Our discussion of the high salt case is scarcely definitive. The problem is that polymer theory does not tell us enough. Polymer segments longer than a persistence length are flexible. Segments shorter than a persistence length resist bending in the manner of a stiff rod. Segments of length of the order of a persistence length possess a mix of both char-

acteristics, but there is no quantitative criterion for the dominance of one over the other.

References

- Ausio, J., Dong, F. & van Holde, K. E. (1989). Use of selectively trypsinized nucleosome core particles to analyze the role of the histone "tails" in the stabilization of the nucleosome. *J. Mol. Biol.* **206**, 451-463.
- Arents, G. & Moudrianakis, E. N. (1993). Topography of the histone octamer surface: repeating structural motifs utilized in the docking of nucleosomal DNA. *Proc. Natl Acad. Sci. USA*, **90**, 10489-10493.
- Borochoy, N., Eisenberg, H. & Kam, Z. (1981). The stiffness of DNA as measured by light scattering. *Biopolymers*, **20**, 231-235.
- Cairney, K. L. & Harrington, R. E. (1982). Flow birefringence of T7 phage DNA: dependence on salt concentration. *Biopolymers*, **21**, 923-934.
- Eisenberg, H. (1990). Thermodynamics and the structure of biological macromolecules. *Eur. J. Biochem.* **187**, 7-22.
- Frontali, C., Dore, E., Ferrauto, A., Gratton, E., Bettini, A., Pozzan, M. R. & Valdevit, E. (1979). An absolute method for the determination of the persistence length of native DNA from electron micrographs. *Biopolymers*, **18**, 1353-1373.
- Hayes, J. J., Tullius, T. D. & Wolffe, A. P. (1990). The structure of DNA in a nucleosome. *Proc. Natl Acad. Sci. USA*, **87**, 7405-7409.
- Manning, G. S. (1981). A procedure for extracting persistence lengths from light scattering data on intermediate molecular weight DNA. *Biopolymers*, **20**, 1751-1755.
- Manning, G. S. (1985). Packaged DNA: an elastic model. *Cell Biophys.* **7**, 177-184.
- Manning, G. S. (1988). An elastic line deformed on a surface by an external field: intrinsic formulation and preliminary application to nucleosome energetics. *Phys. Rev. ser. A*, **38**, 3073-3081.
- Manning, G. S., Ebralidse, K. K., Mirzabekov, A. D. & Rich, A. (1989). An estimate of the extent of folding of nucleosomal DNA by laterally asymmetric neutralization of phosphate groups. *J. Biomol. Struct. Dynam.* **6**, 877-889.
- Marky, N. L. & Manning, G. S. (1991). The elastic resilience of DNA can induce all-or-none structural transitions in the nucleosome core particle. *Biopolymers*, **31**, 1543-1557.
- McGhee, J. D. & Felsenfeld, G. (1980). The number of charge-charge interactions stabilizing the ends of nucleosome DNA. *Nucl. Acids Res.* **8**, 2751-2769.
- Mirzabekov, A. D. & Rich, A. (1979). Asymmetric lateral distribution of unshielded phosphate groups in nucleosomal DNA and its role in DNA bending. *Proc. Natl Acad. Sci. USA*, **76**, 1118-1121.
- Nordmeier, E. (1992). Absorption spectroscopy and dynamic and static light scattering studies of ethidium bromide binding to calf thymus DNA: implications for outside binding and intercalation. *J. Phys. Chem.* **96**, 6045-6055.
- Porschke, D. (1991). Electric dichroism measurements of the persistence length of DNA fragments. *Biophys. Chem.* **40**, 169-179.
- Shore, D. & Baldwin, R. L. (1983). Energetics of DNA twisting. II. Topoisomer analysis. *J. Mol. Biol.* **170**, 983-1007.
- Shrader, T. E. & Crothers, D. M. (1989). Artificial nucleo-

- some positioning sequences. *Proc. Natl Acad. Sci. USA*, **86**, 7418–7422.
- Simpson, R. T. (1979). Mechanism of a reversible, thermally induced conformational change in chromatin core particles. *J. Biol. Chem.* **254**, 10123–10127.
- Sobel, E. S. & Harpst, J. A. (1991). Effects of Na⁺ on the persistence length and excluded volume of T7 bacteriophage DNA. *Biopolymers*, **31**, 1559–1564.
- Strauss, J. K. & Maher, L. J. (1994). DNA bending by asymmetric phosphate neutralization. *Science*, **268**, 1829–1834.
- van Holde, K. E. (1989). *Chromatin*, Springer-Verlag, New York.
- Yager, T. D., McMurray, C. T. & van Holde, K. E. (1989). Salt-induced release of DNA from nucleosome core particles. *Biochemistry*, **28**, 2271–2281.

Edited by B. Honig

(Received 7 April 1995; accepted 14 August 1995)